Case Studies in Thermal Engineering 41 (2023) 102553

Contents lists available at ScienceDirect

Case Studies in Thermal Engineering

journal homepage: www.elsevier.com/locate/csite

Experimental investigation for thermal performance enhancement of various heat sinks using Al_2O_3 NePCM for cooling of electronic devices

Imran Zahid [a,b], M. Farhan [a,**], M. Farooq [a,*], M. Asim [a], M. Imran [c,***]

[a] Faculty of Mechanical Engg., University of Engg. & Technology (UET) Lahore, Pakistan
[b] Department of Mechanical Engg., & Technology, Government College University (GCU) Faisalabad, Faisalabad, Pakistan
[c] Department of Mechanical, Biomedical and Design Engg., College of Engg. and Physical Sciences, Aston University, B4 7ET, Birmingham, UK

ARTICLE INFO

Keywords:
Circular pin-finned
Cu foam
Al_2O_3
RT-54HC (PCM)
Thermal management

ABSTRACT

Electronic devices are being used extensively for different applications, where the thermal management of these devices is still a critical challenge due to rapid miniaturization, high heat flux and constantly rising temperature. Phase change materials (PCMs) based thermal management is adopted, but the low thermal conductivity limits their use in temperature-controlled electronic devices. Nano-enhanced phase change materials (NePCMs) can advance the heat transfer rate (HTr), decrease the temperature, and increase the operating time of the electronic device. The present study compares the thermal performances (TP) of three different heat sinks (simple, circular pin finned and copper foam) with NePCM (RT54HC/Al_2O_3) and varying Al_2O_3 nanoparticles concentrations (0.15–0.25 wt%) and heat fluxes (0.98–2.94 kW/m^2) to optimize the overall device performance. The results show that at a heat flux (HF) of 0.98 kW/m^2 and 0.25 wt % of Al_2O_3 nanoparticles (NPs), the base temperature of simple, circular pin finned and Cu foam heat sink was reduced by 21.3%, 25.03%, and 36.2%, respectively. The Cu foam heat sink (HS) has exceptional TP than the HSs without Cu foam. Accordingly, NePCMs are highly recommended in electronic devices for an optimized thermal management system.

1. Introduction

Electronic components and devices are getting more integrated and rapidly miniaturized, resulting in extremely high-power dissipation rates and constantly rising device temperatures in the modern digital world. So thermal management in electronic technologies is needed to control high heat flux (HF) and increased temperature to secure reliability and durability of device performance and user-level satisfaction [1–3]. Unfortunately, poor thermal management (TM) has caused a shrink in the performance times of several electronic applications, including the Central Processing Unit (CPU), cellular phone, notebooks, control systems in missiles, and printing circuit board (PCBs) [4,5]. According to the survey, 55% of failure in electronics is due to high temperatures beyond working limits [6]. As a result, to improve the cooling efficiency of electronic equipment, the heat generated in electrical circuits must be dispersed rapidly.

* Corresponding author.
** Corresponding author.
*** Corresponding author.
E-mail addresses: m.farhan@uet.edu.pk (M. Farhan), engrfarooq137@gmail.com (M. Farooq), m.imran12@aston.ac.uk (M. Imran).

https://doi.org/10.1016/j.csite.2022.102553
Received 23 April 2022; Received in revised form 3 November 2022; Accepted 10 November 2022
Available online 22 November 2022

Several active and passive electronic cooling methods are adopted for effective TM [7,8]. However, active cooling methods such as nano fluid-based flow circulation and forced air cooling are no longer adequate for efficient thermal management because of noise levels, more space occupancy, additional power requirements, continuous maintenance cost, and pump failures [9–12]. In the numerical investigation, pressure drop and heat transfer parameters were investigated on finned aluminum heat sink with metal foam (MF) under air flow. Fin height, thickness, channel width and length were variable parameters. It was reported that finned MF heat sink performance was outstanding compared with plate finned sink [13]. In order to decrease pumping power and enhance heat transfer, numerical analysis was performed on the finned and unfinned MF heat sink. The heat transfer rate was enhanced using finned MF heat sink from 3.3 to 3.5 times [14].

Passive cooling techniques incorporating phase change materials (PCMs) based heat sinks can show a vital and promising part in electronic chips' thermal performance and operation time [15]. PCMs have innovative features to engross high thermal energy during transient and constant power loads as they melt and solidify at specific temperature ranges (0–100 °C) without any additional power [16,17]. Then it releases heat into the environment to keep the temperature uniform and safe electronic circuits. Although organic PCMs have significant features of chemical stability, noncorrosive, thermophysical properties, thermal diffusivity, latent heat capacity, and low cost [18]. PCMs are now used in building thermal comfort [19], lithium batteries [20], solar thermal systems [21], electronics chips cooling [22], air conditioning systems [23], refrigeration [24], heat pumps [25] and textiles [26]. Low thermal conductivity limits their performances in heat transfer applications.

Therefore, various approaches are studied to increase the thermal performance of PCMs to overcome this limitation [27]. Fig. 1 displays that multiple fins [28–30], nanoparticles [31–33] and foams [5] can be used as thermal performance enhancers with PCMs to overcome thermal conductivity drawbacks.

Extended fins as thermal performance enhancers in heat sinks was the subject of several investigations. Various investigators explored pin finned triangular, circular and rectangular geometries of heat sink filled with PCM as a cooling medium at different input powers. For heat transfer application, triangular geometry of heat sink is suggested to be most promising [34]. The TP of PCM loaded HS with radial extended surfaces has been numerically and experimentally studied to check the effect of ambient and melting temperature at 6 W–10 W. It was observed that the charging time was declined and solidification time was stretched on account of climate temperature difference of 8 °C at the same setpoint temperature (SPT) [35].

Extensive literature has been published on the use of NPs to improve heat transfer and thermal conductivity of PCMs [36]. The experimentally investigated to lift the heat sink's TP by integrating graphene-based nanoparticles into two PCMs of different melting points, lowering the base temperature and increasing the working system's operating time. RT44HC/GNPs and RT64HC/GNPs are recommended for low input power and high heating loads, respectively [37]. The alumina and copper oxide nanoparticles with 2.0%, to 6.0% mass fractions were practiced in a numerical solution of the plate-type finned exchanger. This study reported that adding a small fraction 2% of NPs to pure PCM enhances heat sink performance [38]. Experimentally assessed the influence of carbon nanofibers and titanium oxide NePCMs to observe heat sink performance at 3 W–8 W. The operational time was improved by 110% by the pure cooling media addition in the heat sink at SPT of 35 °C. While adding carbon nanofibers, SPT of 35 °C reduces the running time by 15% [39]. Thermal properties of aluminum oxide PCM-based two different configurations heat sink were evaluated experimentally at mass fractions of 2.0–6.0 wt%. The results showed that NePCM with a lower mass fraction of NPs is desirable for heat sinks performance with investigated parameters [40].

Porous materials' wide surface areas and high thermal conductivities improve PCM heat transfer rates. Several experimental and numerical simulation studies have been conducted using porous material and its composite in heat sink assembly. PCM's transient performance with copper foam heat sinks were studied. According to study findings, 2/3 partial filling metallic foam heat sink with PCM is thermally feasible to achieve comprehensive performance and cost-effective than complete filling [41]. PCM and copper foam-embedded finned heat sink has been numerically investigated to maximize operating time and minimize the cost of the system [42]. Thermal management of electronic components was studied numerically and experimentally using the aluminum (Al)

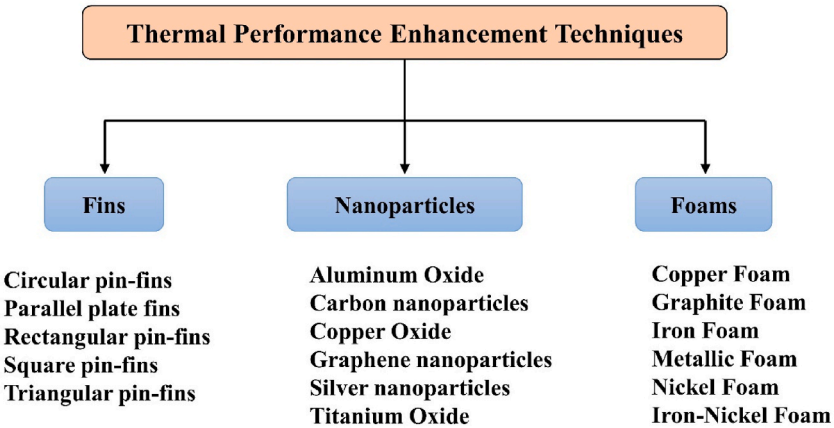

Fig. 1. Thermal performance enhancement techniques of PCMs [25–32].

foams-based composite PCM cylindrical heat sink. Solidity & pores per inch (PPI) parameters are shaped with the vertical pattern of Al-foam slices. Porosity and PPI play a significant role during the charging process but don't affect discharge performance [43]. Table 1 summarizes the results of experimental studies on PCM/NePCM-based heat sinks conducted by various researchers.

It is evident from the literature presented in Table 1 that PCM/NePCM-based heat sinks (HS) have become increasingly desirable in the thermal management of electronics in recent years. However, several studies have only described the effect of heat sink geometry, with a few focusing on metallic foams and NePCM based-simple heat sinks. As for as author's awareness, no study as been carried out by taking all variables, such as simple heat sink without fins, circular fins, copper foam and alumina NePCM sink. NePCM is inserted in the sink for thermal analysis throughout the dissipation and cooling processes of 75 min each. Conducting more extensive experimental research with nano-PCM based various heat sinks would help to understand the requirements for faster passive cooling. Therefore, the present study investigated the combined thermal impact of simple, circular pin-finned and metallic foam heat sinks with RT54HC/Al_2O_3 of various concentrations for different heating loads. Furthermore, the perfomance times of NePCM sinks with set operating conditions were compared with the empty simple heat sink.

2. Experimental

2.1. Research setup

Fig. 2 represnts the arrangement used in this study for the TM performance which consists of various components besides a stable DC voltage regulator and computer. Heat sink assemblage with the internal cavity 101 × 101 × 27 mm^3 comprises simple, circular pin finned and copper foam based heat sinks. In addition, a silicon rubber plate heater (101 × 101 × 1.2 mm^3) was pasted at the base of heat sinks through the thermal paste. It was provided voltage by DC power supply to maintain three different heat fluxes. The base fluctuation in temperature and various points inside the cavity were recorded with the support of thermocouples.

2.2. Design of heat sink

The experimental setup used simple, circular pin-finned and copper foam-incorporated aluminum (Al-6061-T6) heat sinks. Aluminum-based heat sinks were preferred due to corrosion resistance, reasonable thermal conductivity, & lightweight. The current research activity shows that the overall cavity of the heat sink (116 × 116 × 32 mm^3) with 7.5 mm wall thickness is kept constant with volume shares (γ) of nine percent as thermal conductivity enhancers (TCEs). It is the relation among the portion engaged by fins (V_{TCE}) and the empty sink (Vs). The following relation is used to compute the volume shares of TCEs

$$\gamma = \frac{V_{TCE}}{V_s} \tag{1}$$

A CNC equipmets were performed to machine the circular-shaped finned heat sink of 3 mm diameter. Fig. 3 represents ivarious perspectives of the circular finned HS. Each side of the heat sinks was insulated. To maintain a unidirectional heat flow, a cupric sheet was used by the upper boundary of the sink.

The Cu foam with 92% porosity is washed with ethanol, acetone and water before use. The properties of Cu foam is illustrated in Table 2. Fig. 4 illustrates views of three heat sink configurations used for the current experimental study. However, thermal resistance with walls of the heat sink and air gaps within foam/PCM are considered negligible.

2.3. Thermocouples positions

Eleven highly sensitive K-type thermocouples were calibrated and installed at base and different vertical positions to estimate the fluctuations [37]. The error during calibration was found to be ±0.1 °C. The diameter of eight thermocouples was 0.25 mm and of the

Table 1
Literature review on different heat sinks for electronic cooling applications.

Sr. No.	PCM and Melting Point (°C)	NPs Mass Fractions (wt%)	Sonication Time (min)	Heat Flux (kW/m^2)	Dimensions (mm^3)	Metallic Foams	Heat Sink Type	Ref.
1	Paraffin Wax (58–62)			2 and 2.7	100 × 100 X 22		Simple Pin fin	[44]
2	RT-35HC (34–35)			1.58,2 & 2.5	100 × 100 X 50	Cu foam	Simple Heat Pipe	[45]
3	Paraffin Wax (45–47)			0.8,1.6 & 2.4	100 × 100 X 25	Cu foam	Simple	[46]
4	Lauric acid (42–44)			2, 2.6 & 3.2	120 × 120 X 35	Cu foam	Plate fins	[47]
5	Paraffin Wax (59.6)	Graphene 0.05 to 0.5	60	5.6,8.5 & 11.3	42 × 42 X 32		Pin fin	[48]
6	RT-44HC (43–44) RT-64HC (62–64)	Graphene 0.002, 0.005 & & 0.008	180	0.86, 1.44 & 2.4	102 × 102 X 25		Simple	[37]
7	Paraffin Wax (58–62)	CuO	240	1.5 & 3.0	101 × 101 X 25		Simple Circular Triangular	[49]
8	Paraffin Wax (58)	MWCNTs Al_2O_3 2,4 & 6	120		50 × 50 X 50		Simple	[50]

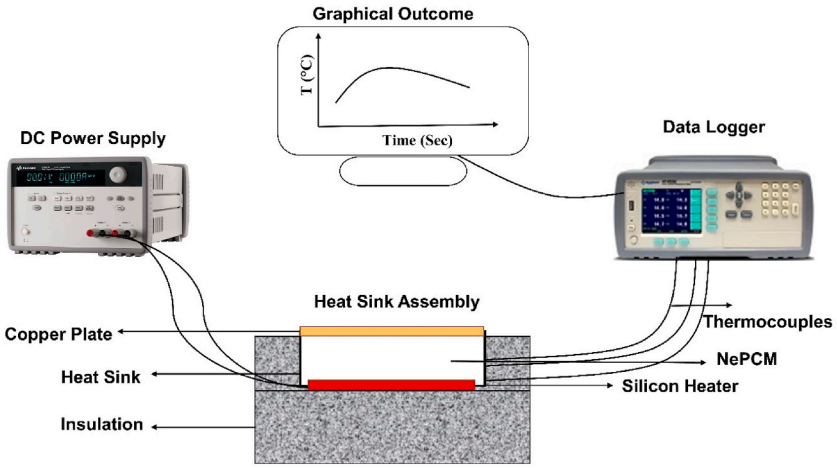

Fig. 2. Experimental apparatus used in current study.

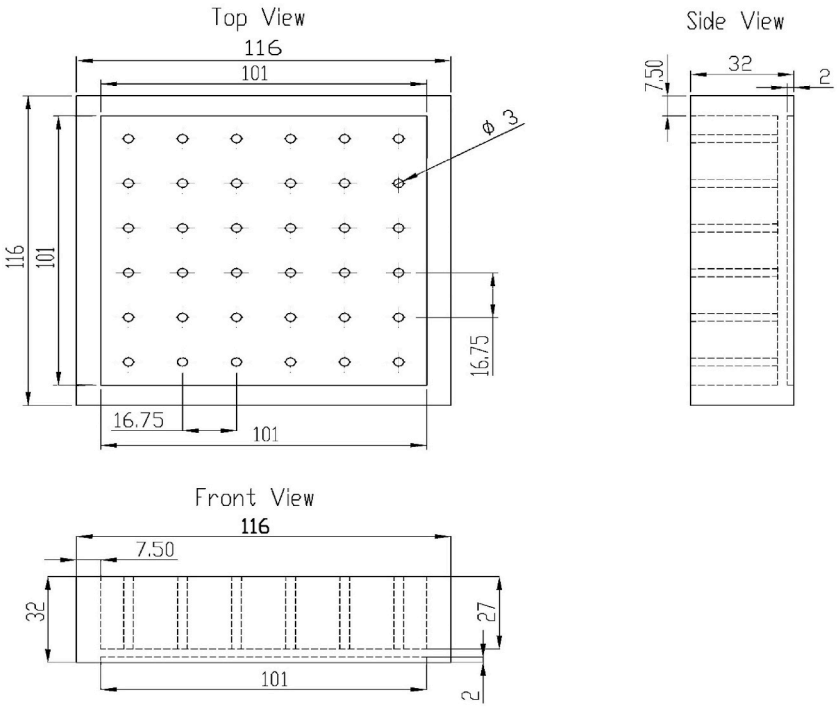

Fig. 3. Various perspective views of the circular shaped HS.

Table 2
Cu foam characteristics.

Material Type	Purity	Density (Kg/m^3)	Pore per inch (PPI)	Porosity (%)	Thermal conductivity (W/m.K)	Cp (KJ/Kg.K)
Cupric Foam	>99	321	25	92	395	0.38

remaining three was 0.50 mm. In addition, the heat sink assembly was made leak-proof using Araldite epoxy to fix the thermocouples. The thermocouples B_1–B_2 were set at the junction of the lower cavity of the sink and the upper face of the square rubber plate heater. The thermocouples V_3–V_{10} were placed in the NePCM at different vertical positioning inside the heat sink. T_{11} was utilized to observe the ambient temperature. Table 3 summarizes the particular positions of thermocouples. The base temperature was measured by the averaging temperature of two thermocouples mounted over the rear cavity of the sink.

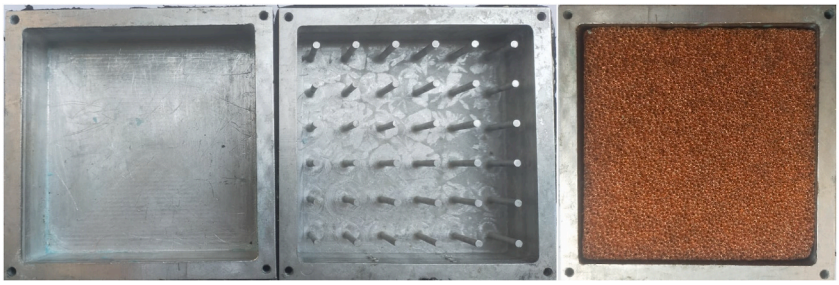

Fig. 4. Pictorial views of simple, circular pin-fin and copper foam-based heat sinks.

2.4. Preparation of NePCM samples

Organic paraffin RT-54HC of 53–54 °C melting temperature was used to quantify the thermal conductance of heat sinks. Table 4 shows the properties of the tested PCM. Aluminum oxide (Al_2O_3) NPs were chosen due to their growth potential in heat transfer applications, enhanced thermophysical properties and better dispersion stability at reasonably low prices [51–53]. A scanning electron microscope (SEM) is commonly used for the size, structure and morphology of NPs. Similarly, an energy dispersive X-ray (EDX) spectrometer is employed to find the weight percentage of NPs element composition. This study used SEM, coupled with EDX, to chemicalize Al_2O_3 NPs, as illustrated in Fig. 5. Firstly, RT-54HC was melted at its melting temperature. Then, to prepare the NePCM mixture, Al_2O_3 NPs of various concentrations were added into melted cooling media, respectively. The mixture is stirred continuously and temperature is maintained at 65 °C, above PCM liquefied temperature. After that blend is processed through ultrasonication for 2 h before using the final mixture. After each test, the quality of PCM was checked and no sign of sedimentation was found.

3. Authentication of experimental setup for TP of sink

The experimental setup was validated by considering previously applied conditions in the published study about empty heat sink base temperature profile before analyzing the results. The majority of research used a heat sink with a dimension of 100 × 100 × 25 mm^3 and HF from 0.0 to 2.6 kW/m^2. In addition, researchers used with and without paraffin wax heat sink for setup validation. To analyze reliability of setup, the empty heat sink base temperature results at 1.58 kW/m^2 obtained from the present test data were compared with Tariq et al. [37] as revealed in Fig. 6.

All boundary of the sink walls are shielded to control dissipation of heat. Therefore, perfect tight insulation covering is assumed to avert any heat removal from the system. Appropriate variables to estimate uncertainties in heat flux (q) can be determined as

$$q = g(V, I, A) \tag{2}$$

Where, $A = g(l \times w)$

The voltage (V), current (I) and length (heating surfaces) inaccuracies are computed.

So fractional uncertainty in terms of applied heat flux will be

$$\frac{\partial q}{q} = \sqrt{(Y_v\,\delta V)^2 + (Y_I\,\delta I)^2 + (Y_l\,\delta l)^2 + (Y_w\,\delta w)^2} \tag{3}$$

Also

$$Y_{v=}\frac{\frac{\partial q}{\partial V}}{q}, Y_I = \frac{\frac{\partial q}{\partial I}}{q}, Y_l = \frac{\frac{\partial q}{\partial l}}{q}, Y_W = \frac{\frac{\partial q}{\partial w}}{q}$$

4. Results and discussions

4.1. Relation of base temperature with PCM/NePCM for different heat sinks

Fig. 7(a) presents the base temperature of warmth exchanger configurations at a HF of 0.98 kW/m^2 (HF-1), using PCM (RT-54HC) for simple heat sink and NePCM (RT54HC/Al_2O_3) for all investigated sinks of various concentrations of Al_2O_3 NPs. The base temperature profile corresponding to the empty heat sink is taken as a reference for other PCM/NePCM based heat sink geometries, as reflected in Fig. 7(a)–(c). The temperature of the simple HS in the absence of PCM/NePCM is 76.39 °C through the melting operation as revealed in Fig. 7(a). The rapid hype in base temperature may lead to failure of electronic components and the problem can be addressed by integrating the subject PCM/NePCMs. The maximum base temperature of a simple warm exchanger reached 64.09 °C

Table 3
Position located on vertical heights.

Thermocouples	B_1–B_2	V_3–V_4	V_5–V_6	V_7–V_8	V_9–V_{10}	T_{11}
Positions (mm)	Heat sink Base	0	9	18	27	Ambient

Table 4
Features of PCM.

Material	Melting temperature (°C)	Density (Kg/m^3)	Thermal conductivity (W/m.K)	Max. operating temperature (°C)	Heat storage capacity (KJ/Kg)	Specific heat (KJ/Kg.K)
RT-54HC	53–54	0.85 (Solid)	0.2	85	200	2

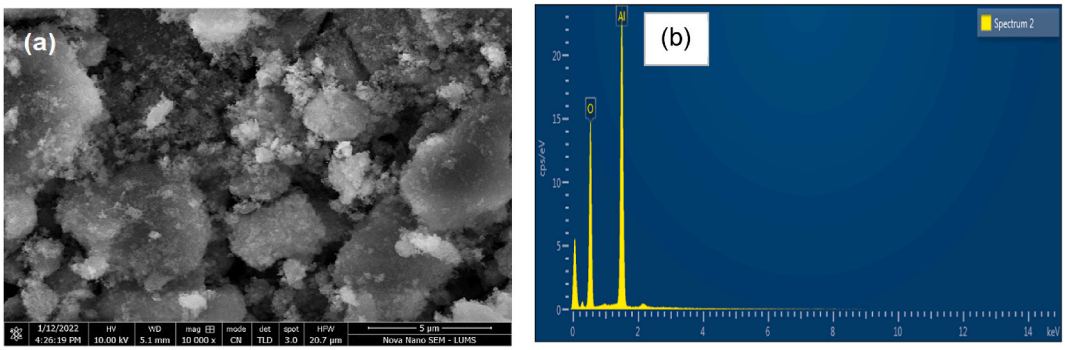

Fig. 5. (a) SEM analysis of Al_2O_3 (b) EDX analysis of Al_2O_3.

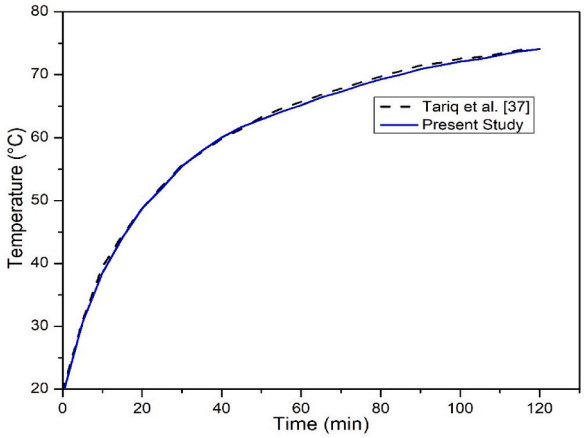

Fig. 6. Experimental setup validation with existing study base temperature.

with the insertion of pure PCM, which is a 16% reduction related to the simple empty sink. The temperature profile of PCM shows a sudden rise, 52 °C, during the first 33 min of charging due to the fact of sensible heating, as shown in Fig. 7(a). After that, the temperature stabilizes slightly in latent heating before post-sensible heating start.

With the addition of 0.15 wt% of Al_2O_3 NPs into PCM, the base temperature of simple, circular pin finned and copper foam heat sink reduced to 20.07%, 24.12% and 32.5%, respectively. Cu foam heat sink showed maximum temperature reduction, i.e. 55.54 °C, because of good thermophysical properties compared to circular pin finned and simple heat sinks. The circular pin finned heat sink reduced the temperature to 57.96 °C, which is slightly improved compared to a simple heat sink filled with NePCM, which is 61.03 °C. The promising results for simple, circular pin-finned and Cu foam heat sinks were achieved by increasing Al_2O_3 NPs with 0.20 wt% and declining the base temperature to 20.6%, 24.3% and 35.12%, respectively. Increasing the NPs to 0.25 wt% resulted in a 21.3%, 25.03%, and 36.2% deplete in the highest sink's base temperature, accordingly.

For input HF of 1.96 kW/m^2 (HF-2)the base profile of various heat sinks is reflected in Fig. 7(b). The empty simple heat sink base temperature goes to 84.3 °C in 75 min of charging time. The simple heat sink filled with PCM has achieved 3% lower base temperature for HF-2 compared to HF-1. At varying concentrations of NPs in PCM, each of the three heat sinks follows a relatively narrow temperature trend with a difference of 1 °C. The percentage drop in base temperature at HF-2 is lesser than the temperature reduction at a HF-1 and high NPs composites. This is because of high heat flux completely melts PCM composites, and post-sensible heating commences after that. Nanoparticles clump together at fully melted paraffin composites, limiting thermophysical characteristics and lowering the drop in base temperature.

Fig. 7(c) illustrates PCM's charging and discharging behavior and its composites with 0.15 wt% to 0.25 wt% Al_2O_3 NPs, imparted in the various heat sinks at a 2.94 kW/m^2 heat flux (HF-3). With 0.15 wt% NePCM, Cu foam heat sinks showed the best thermal performance with a 17.04% temperature drop at the subject heat flux. On the other hand, simple and circular pin finned heat sinks showed 13.15% and 14.06% decrement in base temperature, respectively. The maximum deviation in the base temperature drop is observed 14.83%, 15.73% and 18.65% for simple, circular pin finned and Cu foam heat sinks, respectively, at 0.25 wt% of NPs. Again, the rapid melting of paraffin wax composites, NPs accumulation at the base causes the proportion of base temperature to decrease. At subject applied heat flux, using Al_2O_3 NPs as a heat transfer medium in a Cu foam sink was effective, but oxidation of Cu foam occurred, limiting its use in combination for the thermal management.

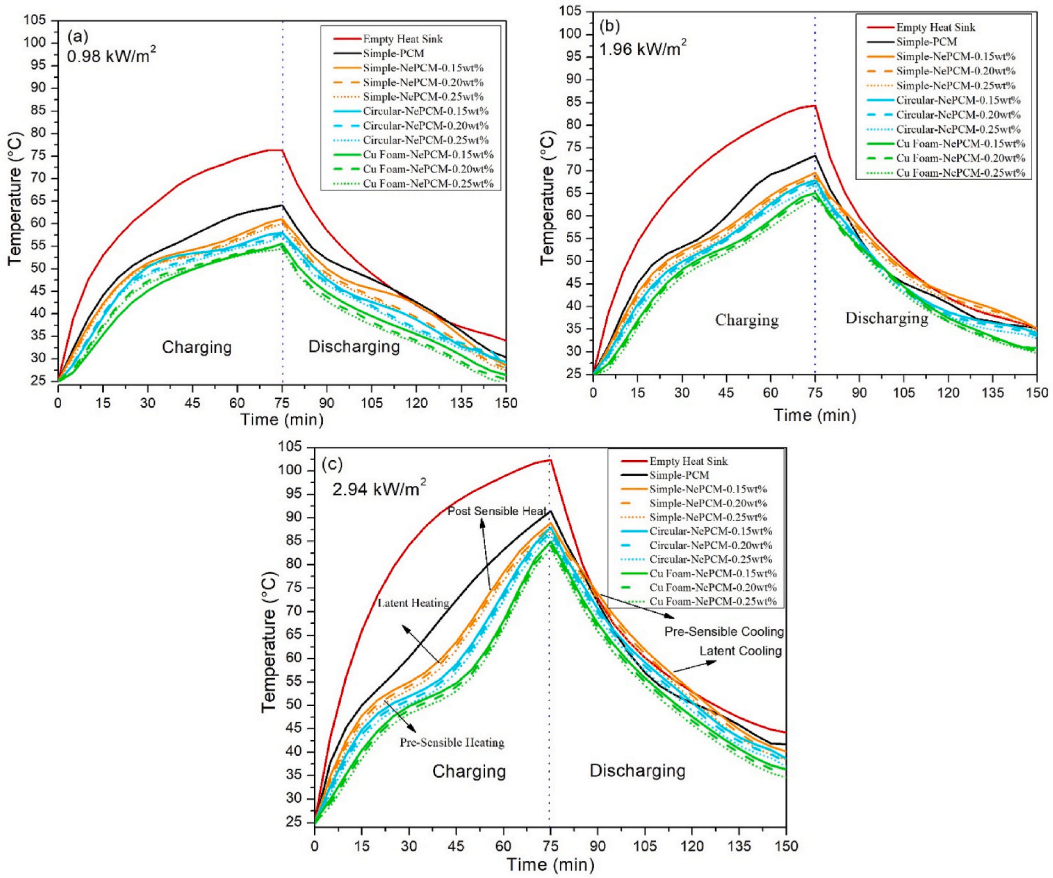

Fig. 7. Comparison of base temperature distribution at HF (a) HF-1 (b) HF-2 (c) HF-3.

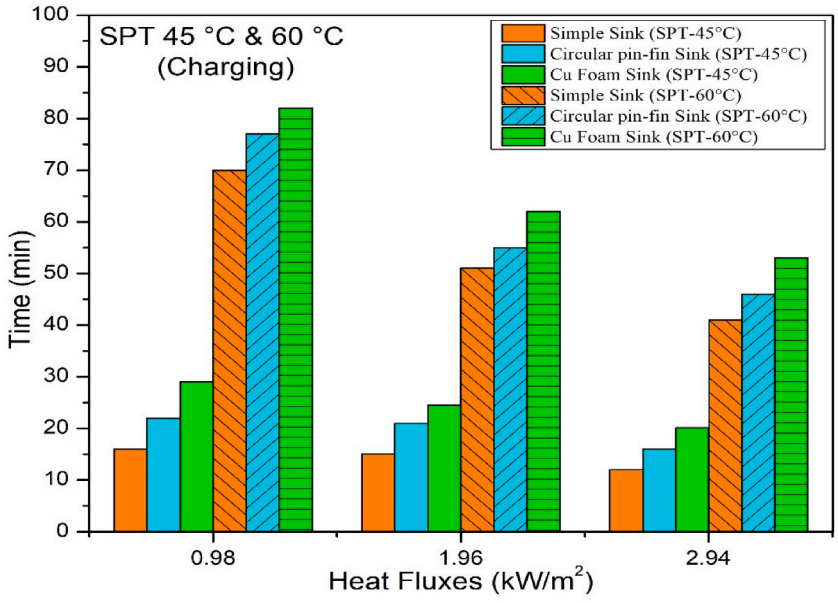

Fig. 8. Comparison of operational time at SPT of 45 °C and 60 °C for various heat sink configurations.

4.2. Analysis of operational time with various setpoint temperatures (SPT)

Setpoint temperature (SPT) is the highest functioning design temperature at which electronic equipment may sustain without losing performance and is also known as critical operating temperature. Two SPTs were selected to examine the TP enrichment in the heat sinks (simple, circular pin finned and Cu foam). Two SPTs are conferred to investigate the most effective cooling technique incorporating RT54HC/Al_2O_3 (0.15 wt%) into heat sinks. These setpoint temperatures are selected depending on electronic equipment heat generation.

4.2.1. Charging process

Fig. 8 describes the enrichment in the operational period of various heat sinks during the charging process. At HF-1, a simple heat sink took a minimum of 16 min to achieve 45 °C, while the circular pin finned exhibited 22 min and a copper foam heat sink acquired a maximum time of 29 min to access the desired target. At a HF-2, it is noticed that a simple sink took a minimum operating time to reach said temperature in comparison with the other configurations. At this point, the Cu foam heat sink grabbed a maximum operation time of 24 min, while the circular pin finned sink took SPT of 45 °C in 21 min. Maximum operation duration is when the cooling device can endure its operational work reliably without triggering any damage and losing efficiency. SPT condenses at a high-power level, resulting in base temperature upsurging rapidly. It can be evidenced that at a 2.94 kW/m^2 heat flux, all three heat sinks achieved SPT of 45 °C in shortening times compared to a HF-2 in 12, 16 and 20 min, respectively.

To inspect the credibility of various sinks performances about SPT of 60 °C, the trends at different heat fluxes are also investigated in Fig. 8. At a low HF-1, the simple sink exchanger reached the SPT of 60 °C in 70 min. On the other hand, the remaining heat sinks did not reach SPT of 60 °C in the heating method, which shows heat sink performance's effectiveness in controlling the 60 °C base temperature. The circular pin finned and Cu foam heat sink attained more time than the charging process due to more heat absorbed by PCM during the latent heating phase. For 1.96 kW/m^2 heat flux, SPTs of three heat sinks were achieved in 51, 55 and 62 min, respectively. Similarly, at 2.94 kW/m^2, Cu foam heat sink again gave an excellent performance and reached SPT of 60 °C in a maximum 53 min, while a simple heat sink performed the least effective in cooling.

4.2.2. Discharging process

SPT of 40 °C is chosen to inquire the solidified restoring performance of three heat sinks (simple, circular pin finned and Cu foam) at various heat fluxes during the discharging process presented in Fig. 9. Cu foam heat sink incorporating RT54HC/Al_2O_3 (0.15 wt%) has shown an excellent cooling performance at applied heat fluxes for discharging cycle. At a HF-1, a Cu foam heat sink took a minimum of 24 min to achieve SPT of 40 °C, while a simple heat sink took a maximum of 50 min. The circular pin finned heat sink achieved SPT in 39 min. A similar trend was observed for a HF-2. At HF-3, SPT of 40 °C was attained by three heat sinks in 75, 68 and 59 min, respectively. It is obvious from Fig. 9 that as HF upsurges period to achieve the desired SPT is enhanced because of the high HF applied.

4.3. Comparison of enhancement ratio with SPTs

The enhancement ratio is expressed as the ration between the time duration to attained at SPT by PCM based heat sink and NePCM based sink heat exchanger [44]. Fig. 10 describes the enhancement ratio of simple, circular and Cu foam heat sink configurations at SPTs (45 °C and 60 °C) against applied heat flux values. The enhancement ratios of simple, circular pin finned and Cu foam heat sinks at SPT of 45 °C are 1.19, 1.38 and 1.81 at the HF-1. Similarly, at HF-2, the enhancement ratio of the three heat sinks is 1.24, 1.52 and 1.69, respectively. At a HF-3, enhancement ratios of simple, circular pin finned and Cu foam heat sinks are 1.37, 1.68 and 2.21 times. It becomes evident from Fig. 10 that the Cu foam heat sink showed the maximal enhancement ratio of 5.7 at SPT of 60 °C than other heat sinks at all heat flux.

4.4. Effect on absolute temperature reduction and operating time enhancement

Table 5 comprises the absolute base temperature reduction with the operating time enhancement at various NPs concentrations and heat fluxes for different heat sink configurations. At HF-1, the absolute base temperature of the simple heat sink declined to 15.33 °C, but the operating time increased by 45 min. For circular pin finned and Cu foam heat sinks, the working span of the device is enhanced by 55 min–62 min with 18.43 °C–20.85 °C reductions in base comparison. A similar trend was observed at heat flux of HF-2. But absolute temperature difference and operating duration enhancement declined because of the high heat absorbed by NePCM at HF-2. Compared to a drop in absolute temperature of 13.47 °C, 14.40 °C and 17.45 °C, the working time of simple, circular pin finned, and Cu foam heat sinks was enhanced by 21.50 min, 27.50 min, and 33.50 min, respectively, at 0.15 wt% NPs fractions and heat flux of HF-3. The Cu foam heat sink performed best for the thermal management of electronics at all HF values and 0.25 wt% as shown in Fig. 11.

5. Conclusion

A comparison of configurations of HS (simple, circular pin finned and Cu-foam) filled with NePCM were analysed for passive TM of portable electronic devices/components using different HFs. Some significant outcomes from the above experimental analysis are described below;

- The base temperature profile of the empty heat sink remained leading and higher than all other temperature curves at all three heat fluxes, which may be harmful to electronic components.
- The NePCM insertion and increased concentration of Al_2O_3 NPs regulated the HTr performance and kept the system base temperature within the working range of electronic devices.

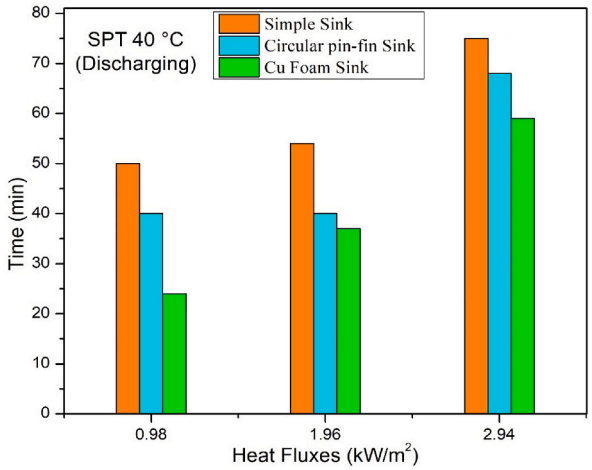

Fig. 9. Behavior of cooling time and hHF at SPT of 40 °C.

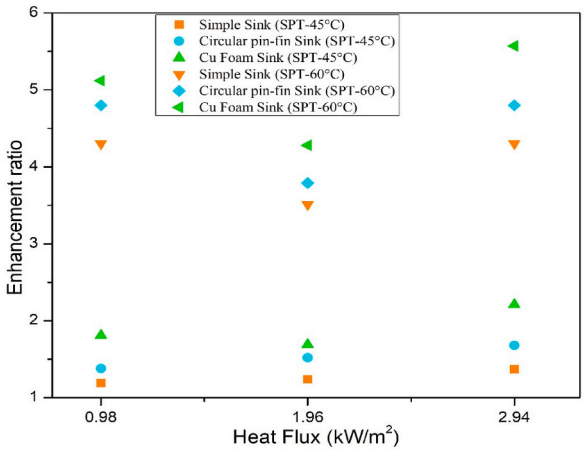

Fig. 10. Enhancement ratio of heat sinks.

Table 5
Comparison of the absolute temperature reduction and operating time enhancement.

		HF-1			HF-2			HF-3		
NPs fractions (wt%)	Difference (°C, min)	Simple HS	Circular HS	Cu foam HS	Simple HS	Circular HS	Cu foam HS	Simple HS	circular HS	Cu foam HS
0.15	Absolute temperature reduction	15.33	18.43	20.85	14.75	16.44	19.15	13.47	14.40	17.45
	Operating time enhancement	45	55	62	30	33.50	42	21.50	27.50	33.50
0.20	Absolute temperature reduction	15.75	18.62	21.45	15.35	17.04	19.79	14.33	15.27	18.28
	Operating time enhancement	48	57	68	31.50	35.30	43.50	23.70	28.80	34.6
0.25	Absolute temperature reduction	16.29	19.13	22.01	15.99	17.50	20.37	15.19	16.11	19.10
	Operating time enhancement	49.50	60	71	33.30	37.40	45.10	25	29.90	35.4

- The aggregation of NPs at higher concentrations resulted in the deterioration of heat transfer rate at high heat flux. However, the overall heat transfer rate increased at all mass percentages of NPs.
- At HF-3 and highest concentration of Al_2O_3, the base temperature of simple, circular pin finned and Cu foam heat sinks was reduced by 13.15%, 15.73%, and 18.65%, respectively.

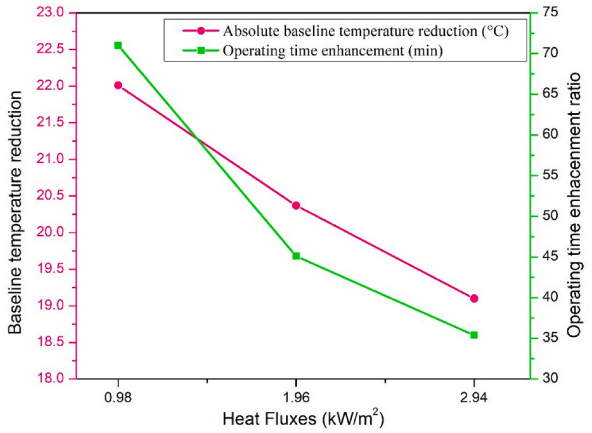

Fig. 11. Relation between absolute reduction in temperature and enhancement in operating duration of Cu foam sink.

- The TP of Cu foam heat sink was stronger preferable than other heat sinks configurations during the charging process in achieving SPTs of 45 °C and 60 °C.
- However, Cu foam can oxidize with Al_2O_3 NPs at the HF-3 and, therefore, is not recommended under subject operating conditions.
- The present investigation also suggests to analyze theTP of other types of foams, such as iron-nickel, aluminum and foams coated with highly conductive materials in different configurations of heat sinks.
- Efforts are also needed to utilize hybrid cooling (active and passive) for a better thermal management of electronic components in future study.

Author credit statement

Imran Zahid: Formulation, Data arrangement, Formal analysis, Procedure, Writing - original draft, Writing - review and editing. Muhammad Farhan: Conceptualization, Investigation, Project administration, Software, Supervision, Writing - review and editing. Muhammad Farooq: Conceptualization, Data organization, Methodology, Project administration, Supervision, Writing - review and editing. Muhammad Asim: Methodology, Validation, Writing - review and editing. Muhammad Imran: Funding acquisition, Project administration, Validation, Writing - inspection and revising.

Declaration of competing interest

The authors declare that they have no known competing financial interests or personal relationships that could have appeared to influence the work reported in this paper.

Data availability

Data will be made available on request.

Acknowledgment

The authors are thankful to the University of Engineering and Technology Lahore for funding through grant No: ORIC/110-ASRB/1641 to execute the current research work.

References

[1] T. Ambreen, A. Saleem, H.M. Ali, S.A. Shehzad, C.W. Park, Performance analysis of hybrid nanofluid in a heat sink equipped with sharp and streamlined micro pin-fins, Powder Technol. 355 (Oct. 2019) 552–563, https://doi.org/10.1016/J.POWTEC.2019.07.087.
[2] M. Sajjad, et al., Effect of various evaluation criteria on heat transfer enhancement of nanofluids: a case study of water-based Cu 2 O nanofluids, Arabian J. Sci. Eng. 45 (3) (2020) 953–966, https://doi.org/10.1007/s13369-019-04187-w.
[3] H.-R. Siddiqi, et al., Heat transfer and pressure drop characteristics of ZnO/DIW based nanofluids in small diameter compact channels: an experimental study, Case Stud. Therm. Eng. 39 (Nov. 2022), 102441, https://doi.org/10.1016/J.CSITE.2022.102441.
[4] R. Viswanath, et al., Thermal Performance Challenges from Silicon to Systems, 2000. Accessed: Feb. 12, 2022. [Online]. Available: http://citeseerx.ist.psu.edu/viewdoc/summary?doi=10.1.1.14.8322.
[5] M. Ghalambaz, J. Zhang, Conjugate solid-liquid phase change heat transfer in heatsink filled with phase change material-metal foam, Jan, Int. J. Heat Mass Tran. 146 (2020), 118832, https://doi.org/10.1016/J.IJHEATMASSTRANSFER.2019.118832.
[6] E.M. Alawadhi, C.H. Amon, Performance analysis of an enhanced PCM thermal control unit, Thermomechanical Phenom. Electron. Syst. -Proceedings Intersoc. Conf. 1 (2000) 283–289, https://doi.org/10.1109/ITHERM.2000.866837.
[7] D. Ouyang, J. Weng, J. Hu, M. Chen, Q. Huang, J. Wang, Experimental investigation of thermal failure propagation in typical lithium-ion battery modules, Thermochim. Acta 676 (Jun. 2019) 205–213, https://doi.org/10.1016/J.TCA.2019.05.002.
[8] A. Arshad, M. Jabbal, Y. Yan, Thermophysical characteristics and application of metallic-oxide based mono and hybrid nanocomposite phase change materials for thermal management systems, Appl. Therm. Eng. 181 (Nov. 2020), 115999, https://doi.org/10.1016/J.APPLTHERMALENG.2020.115999.

[9] A. Taheri, M. Ghasemian Moghadam, M. Mohammadi, M. Passandideh-Fard, M. Sardarabadi, A new design of liquid-cooled heat sink by altering the heat sink heat pipe application: experimental approach and prediction via artificial neural network, Energy Convers. Manag. 206 (Feb. 2020), 112485, https://doi.org/10.1016/J.ENCONMAN.2020.112485.

[10] M. Sajid, I. Hassan, A. Rahman, An overview of cooling of thermoelectric devices, Renew. Sustain. Energy Rev. 78 (Oct. 2017) 15–22, https://doi.org/10.1016/J.RSER.2017.04.098.

[11] Z. Khattak, H.M. Ali, Air cooled heat sink geometries subjected to forced flow: a critical review, Mar, Int. J. Heat Mass Tran. 130 (2019) 141–161, https://doi.org/10.1016/J.IJHEATMASSTRANSFER.2018.08.048.

[12] M. Mohammadi, A. Taheri, M. Passandideh-Fard, M. Sardarabadi, Electronic chipset thermal management using a nanofluid-based mini-channel heat sink: an experimental study, Nov, Int. Commun. Heat Mass Tran. 118 (2020), 104836, https://doi.org/10.1016/J.ICHEATMASSTRANSFER.2020.104836.

[13] S.S. Fen, J.J. Kuang, T.J. Lu, K. Ichimiya, Heat transfer and pressure drop characteristics of finned metal foam heat sinks under uniform impinging flow, Jun, J. Electron. Packag. Trans. ASME 137 (2) (2015), https://doi.org/10.1115/1.4029722/372595.

[14] N. Bianco, M. Iasiello, G.M. Mauro, L. Pagano, Multi-objective optimization of finned metal foam heat sinks: tradeoff between heat transfer and pressure drop, Appl. Therm. Eng. 182 (Jan. 2021), 116058, https://doi.org/10.1016/J.APPLTHERMALENG.2020.116058.

[15] J. Watson, G. Castro, A review of high-temperature electronics technology and applications, Dec, J. Mater. Sci. Mater. Electron. 26 (12) (2015) 9226–9235, https://doi.org/10.1007/S10854-015-3459-4/TABLES/3.

[16] M.R. Attar, et al., Heat transfer enhancement of conventional aluminum heat sinks with an innovative, cost-effective, and simple chemical roughening method, Therm. Sci. Eng. Prog. 20 (Dec. 2020), 100742, https://doi.org/10.1016/J.TSEP.2020.100742.

[17] J. Wang, H. Xie, Z. Guo, L. Guan, Y. Li, Improved thermal properties of paraffin wax by the addition of TiO2 nanoparticles, Appl. Therm. Eng. 73 (2) (Dec. 2014) 1541–1547, https://doi.org/10.1016/J.APPLTHERMALENG.2014.05.078.

[18] C. Veerakumar, A. Sreekumar, Phase change material based cold thermal energy storage: materials, techniques and applications – a review, Jul, Int. J. Refrig. 67 (2016) 271–289, https://doi.org/10.1016/J.IJREFRIG.2015.12.005.

[19] S.L. Tariq, H.M. Ali, M.A. Akram, M.M. Janjua, M. Ahmadlouydarab, Nanoparticles enhanced phase change materials (NePCMs)-A recent review, Appl. Therm. Eng. 176 (Jul. 25, 2020), 115305, https://doi.org/10.1016/j.applthermaleng.2020.115305. Elsevier Ltd.

[20] H. Bashirpour-Bonab, Thermal behavior of lithium batteries used in electric vehicles using phase change materials, Int. J. Energy Res. 44 (15) (Dec. 2020) 12583–12591, https://doi.org/10.1002/ER.5425.

[21] M. He, L. Yang, W. Lin, J. Chen, X. Mao, Z. Ma, Preparation, thermal characterization and examination of phase change materials (PCMs) enhanced by carbon-based nanoparticles for solar thermal energy storage, J. Energy Storage 25 (Oct. 2019), 100874, https://doi.org/10.1016/J.EST.2019.100874.

[22] W. Hua, L. Zhang, X. Zhang, Research on passive cooling of electronic chips based on PCM: a review, J. Mol. Liq. 340 (Oct. 2021), 117183, https://doi.org/10.1016/J.MOLLIQ.2021.117183.

[23] A.A.M. Omara, A.A.A. Abuelnour, Improving the performance of air conditioning systems by using phase change materials: a review, Aug, Int. J. Energy Res. 43 (10) (2019) 5175–5198, https://doi.org/10.1002/ER.4507.

[24] H. Selvnes, Y. Allouche, R.I. Manescu, A. Hafner, Review on cold thermal energy storage applied to refrigeration systems using phase change materials, Therm. Sci. Eng. Prog. 22 (May 2021), 100807, https://doi.org/10.1016/J.TSEP.2020.100807.

[25] S. Rashidi, H. Shamsabadi, J.A. Esfahani, S. Harmand, A review on potentials of coupling PCM storage modules to heat pipes and heat pumps, May, J. Therm. Anal. Calorim. 140 (4) (2020) 1655–1713, https://doi.org/10.1007/S10973-019-08930-1/TABLES/3.

[26] K. Yang, et al., Review: incorporation of organic PCMs into textiles, 2021 572, J. Mater. Sci. 57 (2) (Jan. 2022) 798–847, https://doi.org/10.1007/S10853-021-06641-3.

[27] B. Eanest Jebasingh, A. Valan Arasu, A comprehensive review on latent heat and thermal conductivity of nanoparticle dispersed phase change material for low-temperature applications, Energy Storage Mater. 24 (Jan. 01, 2020) 52–74, https://doi.org/10.1016/j.ensm.2019.07.031. Elsevier B.V.

[28] M.J. Ashraf, H.M. Ali, H. Usman, A. Arshad, Experimental passive electronics cooling: parametric investigation of pin-fin geometries and efficient phase change materials, Int. J. Heat Mass Tran. 115 (Dec. 2017) 251–263, https://doi.org/10.1016/J.IJHEATMASSTRANSFER.2017.07.114.

[29] A. Arshad, H.M. Ali, M. Ali, S. Manzoor, Thermal performance of phase change material (PCM) based pin-finned heat sinks for electronics devices: effect of pin thickness and PCM volume fraction, Appl. Therm. Eng. 112 (Feb. 2017) 143–155, https://doi.org/10.1016/j.applthermaleng.2016.10.090.

[30] K.Y. Leong, S.P. Chew, B.A. Gurunathan, K.Z. Ku Ahmad, H.C. Ong, An experimental approach to investigate thermal performance of paraffin wax and 1-hexadecanol based heat sinks for cooling of electronic system, Int. Commun. Heat Mass Tran. 109 (Dec. 2019), 104365, https://doi.org/10.1016/J.ICHEATMASSTRANSFER.2019.104365.

[31] L. Yang, J. nan Huang, F. Zhou, Thermophysical properties and applications of nano-enhanced PCMs: an update review, Energy Convers. Manag. 214 (April) (2020), 112876, https://doi.org/10.1016/j.enconman.2020.112876.

[32] M. Farooq, et al., Thermal performance enhancement of nanofluids based parabolic trough solar collector (NPTSC) for sustainable environment, Alex. Eng. J. 61 (11) (Nov. 2022) 8943–8953, https://doi.org/10.1016/J.AEJ.2022.02.029.

[33] M. Ijaz, et al., Numerical investigation of particles characteristics on cyclone performance for sustainable environment, Part. Sci. Technol. 39 (4) (2021) 495–503, https://doi.org/10.1080/02726351.2020.1768610.

[34] H.M. Ali, et al., Thermal management of electronics: an experimental analysis of triangular, rectangular and circular pin-fin heat sinks for various PCMs, Int. J. Heat Mass Tran. 123 (Aug. 2018) 272–284, https://doi.org/10.1016/J.IJHEATMASSTRANSFER.2018.02.044.

[35] G.K. Marri, R. Srikanth, C. Balaji, Effect of phase change and ambient temperatures on the thermal performance of a solid-liquid phase change material based heat sinks, J. Energy Storage 30 (Aug. 2020), 101327, https://doi.org/10.1016/J.EST.2020.101327.

[36] M. Aurangzeb, et al., Investigation of enhancement in the thermal response of phase change materials through nano powders, Case Stud. Therm. Eng. 29 (Jan. 2022), 101654, https://doi.org/10.1016/J.CSITE.2021.101654.

[37] S.L. Tariq, H.M. Ali, M.A. Akram, M.M. Janjua, Experimental investigation on graphene based nanoparticles enhanced phase change materials (GbNePCMs) for thermal management of electronic equipment, J. Energy Storage 30 (Aug. 2020), 101497, https://doi.org/10.1016/j.est.2020.101497.

[38] M. Bayat, M.R. Faridzadeh, D. Toghraie, Investigation of finned heat sink performance with nano enhanced phase change material (NePCM), Mar, Therm. Sci. Eng. Prog. 5 (2018) 50–59, https://doi.org/10.1016/J.TSEP.2017.10.021.

[39] S. Motahar, R. Khodabandeh, An experimental assessment of nanostructured materials embedded in a PCM-based heat sink for transient thermal management of electronic, Jul, Challenges Nano Micro Scale Sci. Technol. 6 (2) (2018) 96–103, https://doi.org/10.22111/TPNMS.2018.22225.1133.

[40] R. Kothari, S.K. Sahu, S.I. Kundalwal, Investigation on thermal characteristics of nano enhanced phase change material based finned and unfinned heat sinks for thermal management system, Chem. Eng. Process. - Process Intensif. 162 (May 2021), 108328, https://doi.org/10.1016/J.CEP.2021.108328.

[41] Z.Q. Zhu, Y.K. Huang, N. Hu, Y. Zeng, L.W. Fan, Transient performance of a PCM-based heat sink with a partially filled metal foam: effects of the filling height ratio, Jan, Appl. Therm. Eng. 128 (2018) 966–972, https://doi.org/10.1016/J.APPLTHERMALENG.2017.09.047.

[42] N. Bianco, S. Busiello, M. Iasiello, G.M. Mauro, Finned heat sinks with phase change materials and metal foams: pareto optimization to address cost and operation time, Oct, Appl. Therm. Eng. 197 (2021), https://doi.org/10.1016/J.APPLTHERMALENG.2021.117436.

[43] G.K. Marri, C. Balaji, Experimental and numerical investigations on the effect of porosity and PPI gradients of metal foams on the thermal performance of a composite phase change material heat sink, Int. J. Heat Mass Tran. 164 (Jan. 2021), 120454, https://doi.org/10.1016/J.IJHEATMASSTRANSFER.2020.120454.

[44] R. Kothari, S.K. Sahu, S.I. Kundalwal, P. Mahalkar, Thermal performance of phase change material–based heat sink for passive cooling of electronic components: an experimental study, Int. J. Energy Res. 45 (4) (Mar. 2021) 5939–5963, https://doi.org/10.1002/ER.6215.

[45] M.A. Hayat, H.M. Ali, M.M. Janjua, W. Pao, C. Li, M. Alizadeh, Phase change material/heat pipe and Copper foam-based heat sinks for thermal management of electronic systems, J. Energy Storage 32 (Dec. 2020), 101971, https://doi.org/10.1016/J.EST.2020.101971.

[46] T. ur Rehman, H.M. Ali, Experimental investigation on paraffin wax integrated with copper foam based heat sinks for electronic components thermal cooling, Int. Commun. Heat Mass Tran. 98 (September) (2018) 155–162, https://doi.org/10.1016/j.icheatmasstransfer.2018.08.003.

[47] Y. Huang, Q. Sun, F. Yao, C. Zhang, 7, in: Experimental Study on the Thermal Performance of a Finned Metal Foam Heat Sink with Phase Change Material, vol. 42, 2020, pp. 579–591, https://doi.org/10.1080/01457632.2020.1716482, 10.1080/01457632.2020.1716482.
[48] M. Joseph, V. Sajith, Graphene enhanced paraffin nanocomposite based hybrid cooling system for thermal management of electronics, Appl. Therm. Eng. 163 (Dec. 2019), 114342, https://doi.org/10.1016/J.APPLTHERMALENG.2019.114342.
[49] A. Kumar, R. Kothari, S.K. Sahu, S.I. Kundalwal, Thermal performance of heat sink using nano-enhanced phase change material (NePCM) for cooling of electronic components, Microelectron. Reliab. 121 (Jun. 2021), 114144, https://doi.org/10.1016/J.MICROREL.2021.114144.
[50] M. Aqib, A. Hussain, H.M. Ali, A. Naseer, F. Jamil, Experimental case studies of the effect of Al2O3 and MWCNTs nanoparticles on heating and cooling of PCM, Case Stud. Therm. Eng. 22 (Dec. 2020), 100753, https://doi.org/10.1016/J.CSITE.2020.100753.
[51] T.A. Khan, H. Ahmad, CFD-based comparative performance analysis of different nanofluids used in automobile radiators, 446, Arabian J. Sci. Eng. 44 (6) (2019) 5787–5799, https://doi.org/10.1007/S13369-019-03750-9. Feb. 2019.
[52] H.M.A. Hassan, et al., Performance analysis of nanofluid-based water desalination system using integrated solar still, flat plate and parabolic trough collectors, Sep, J. Brazilian Soc. Mech. Sci. Eng. 44 (9) (2022), https://doi.org/10.1007/S40430-022-03734-1.
[53] A. Qamar, et al., Preparation and dispersion stability of aqueous metal oxide nanofluids for potential heat transfer applications: a review of experimental studies, J. Therm. Anal. Calorim. 147 (1) (Jan. 2022) 23–46, https://doi.org/10.1007/S10973-020-10372-Z.